 doi:10.20944/preprints202201.0199.v1

Article

A Generalized Construction Model for CT Reconstruction Filters on the SDBP Technique

Yi-ming Jiang [1], Jin-tao Zhao [2], Xiao-dong Hu [1] and Jing Zou [1,*]

[1] School of Precision Instrument and Opto-Electronics Engineering, Tianjin University, Tianjin 300072, China; ymjiang@tju.edu.cn
[2] Tianjin Key Laboratory of Information Sensing and Intelligent Control, Tianjin University of Technology and Education, Tianjin 300222, China; zjt2019@tju.edu.cn
* Correspondence: jingzoutd@tju.edu.cn

Abstract: As an implementation of inverse Radon transform, the Second-order Divided-difference Back Projection (SDBP) technique has been proposed in this paper, by which the accurate CT reconstruction can be theoretically realized. A computational model for CT reconstruction filter expressions has been derived on the basis of SDBP technique. The method reveals the correlation between the convolution kernel for data restoration and the filter expression. By substituting kernel functions into the computational model, the amplitude sequences of a variety of filters can be calculated. On the proposed filter construction method, the decomposition form of filters has been discovered, where a series of basic filters have been acquired. The properties of any filter depend on the decomposed basic filters. Basic filters can be used to compose filters in actual needs.

Keywords: inverse Radon transform; CT; SDBP; filter design; kernel function; Hilbert transform; basic filters

1. Introduction

Computed tomography (CT) technology is a commonly used nondestructive testing method [1,2]. Techniques related to reconstruction algorithms are the research focuses in the field of CT imaging. In the view of mathematical analysis, the CT reconstruction is essentially an inverse problem of the Radon transform [3]. Therefore, the properties of Radon transform have always been the research topic in the CT field [4-6]. Among all algorithms based on the inverse Radon transform, the filtered back projection (FBP) technique is a typical case [7], which is efficient and convenient to implement. However, due to the divergence of the ideal ramp function, FBP technique can not be equivalent to the rigorous Radon inverse transform. An accurate and effective inverse Radon transform method is essential to the theoretical research of CT reconstruction. On the known derivation process, this paper has proposed an inverse Radon transform formula in the form of second-order divided-difference back projection (SDBP). Different from FBP technique, SDBP technique calculates the functional second-order difference instead of filtering in the projection data preprocessing. Theoretically, SDBP is an accurate reconstruction method for dense sampling.

For discrete projection data, the performance of the CT reconstruction filter is an important factor that affects CT image quality. Presently, the most commonly used filters in FBP are R-L filter [8] and S-L filter [9]. The CT image reconstructed by R-L filter has clear contour and high spatial resolution, but the image is affected by obvious Gibbs phenomenon [10]. Compared with R-L filter, the CT image reconstructed by S-L filter has lighter Gibbs phenomenon and less grayscale error, but the sharpness of the contour edge is lower. Not all filters can be obtained by the traditional design method, which is realized by inverse Fourier transform after windowing the ramp function in frequency domain.

Preprints (www.preprints.org) | NOT PEER-REVIEWED | Posted: 14 January 2022 doi:10.20944/preprints202201.0199.v1

For that reason, scholars have also studied some designing methods of CT reconstruction filters [11-13].

In this paper, a generalized construction model of CT reconstruction filters has been proposed. It begins with the discrete projection data being restored into a continuous function by convolution with kernel function. By applying the SDBP formula to the restored second-order difference projection function, the relationship between the filter function and the kernel function has been revealed. As an application, a variety of filters can be acquired by applying different kernel functions to the proposed model. In particular, R-L filter and S-L filter can be acquired respectively with sinc kernel and rectangular kernel. Based on the derived theorem, it has been proved that any filter can be decomposed into a linear combination of basic filters. Through simulations of CT reconstruction for the Shepp-Logan phantom, some characteristics of the basic filters have been demonstrated, which provide guidance for the filter design. This study has provided a theoretical foundation for the analysis of CT reconstruction filters.

2. Inverse Radon Transform with SDBP Technique

SDBP technique is a method for realizing inverse Radon transform. For the projection data sets of linear continuum, SDBP technique is a practicable way to achieve accurate analytical reconstruction of the target function. SDBP technique also provides an approach for CT reconstruction with discrete sinogram, even if the sampling is not equidistant.

2.1. Radon Transform

Each $\bullet$ refers to a variable, and each $\otimes$ refers to a function. Given a target real function $f(\bullet)$, for $\vec{x}=(x,y)^T\in\mathbb{R}^2$, assume that $f(\vec{x})$ satisfies the following conditions:

Hypothesis 1.

1. $f(\vec{x})$ is continuous;
2. The double integral $\iint\frac{|f(\vec{x})|}{\sqrt{\vec{x}^T\vec{x}}}\mathrm{d}^2\vec{x}$ extending over the whole plane, converges;
3. For any arbitrary point $\vec{x}$ on the plane, $\lim\limits_{\varepsilon\to 0_+}\int_0^{2\pi}f\left(\vec{x}+\frac{\vec{\varphi}}{\varepsilon}\right)\mathrm{d}\varphi=0$, where $\vec{\varphi}=(\cos\varphi,\sin\varphi)^T$.

Definition 1. The Radon transform of $f(\vec{x})$ is a linear integral transform in the plane [3], which is defined as

$$\mathcal{R}[f](r,\varphi):=\int_{\mathbb{R}}f(r\vec{\varphi}+\tau\vec{\varphi}_\perp)\mathrm{d}\tau, \tag{1}$$

where, r is the distance of straight line $\{L:\vec{\varphi}^T\vec{x}-r=0\}$ from the origin; $\vec{\varphi}_\perp=(\sin\varphi,-\cos\varphi)^T$.

The Radon transformed functions defined in equation (1) and the original functions constitute a function space of bijections.

2.2. SDBP Technique

For $r\in\mathbb{R}$ and $\varphi\in(0,2\pi]$, given the Radon transform $\mathcal{R}[f](r,\varphi)$ of the target function $f(\vec{x})$ to be solved, assume that $\mathcal{R}[f](r,\varphi)$ satisfies the following conditions:

Preprints (www.preprints.org) | NOT PEER-REVIEWED | Posted: 14 January 2022 doi:10.20944/preprints202201.0199.v1

Hypothesis 2.

1. The integral $\int_{\mathbb{R}}\left|\mathcal{R}[f](r,\varphi)\right|\mathrm{d}r$ converges;
2. $\lim\limits_{s\to 0}\Delta_r^2\left[\mathcal{R}[f](r,\varphi)\right](s)=0$, where $\Delta_r^2[\otimes](s)$ of $s\in\mathbb{R}$ is the second-order difference operator for variable r, and more specifically

$$\Delta_r^2\left[\mathcal{R}[f](r,\varphi)\right](s):=\mathcal{R}[f](r-s,\varphi)-2\mathcal{R}[f](r,\varphi)+\mathcal{R}[f](r+s,\varphi);$$

3. The first partial derivative $\frac{\partial}{\partial r}\mathcal{R}[f](r,\varphi)$ is continuous, or only has removable discontinuities;
4. The second partial derivative $\frac{\partial^2}{\partial r^2}\mathcal{R}[f](r,\varphi)$ is continuous , or only has removable or jump discontinuities.

On the premise of the Radon transform $\mathcal{R}[f](r,\varphi)$ meeting **Hypothesis 2**, the formula of SDBP technique for inverse Radon transform is shown as follows:

Theorem 1. For $\vec{\boldsymbol{x}}\in\mathbb{R}^2$, $r\in\mathbb{R}$, $s\in\mathbb{R}$, $\varphi\in[0,2\pi)$,

$$f(\vec{\boldsymbol{x}})=-\frac{1}{4\pi^2}\lim_{\varepsilon\to 0_+}\int_0^{2\pi}\int_{\varepsilon}^{+\infty}\left.\frac{\Delta_r^2\left[\mathcal{R}[f](r,\varphi)\right](s)}{s^2}\right|_{r=\vec{\boldsymbol{\varphi}}^T\vec{\boldsymbol{x}}}\mathrm{d}s\mathrm{d}\varphi. \tag{2}$$

If $s\to 0$, the integrand is equal to the mean value of second partial derivatives of $\mathcal{R}[f](r,\varphi)$ on both sides of the index position, as

$$\lim_{s\to 0}\frac{\Delta_r^2\left[\mathcal{R}[f](r,\varphi)\right](s)}{s^2}=\frac{1}{2}\left(\frac{\partial^2}{\partial r^2}\mathcal{R}[f](r_+,\varphi)+\frac{\partial^2}{\partial r^2}\mathcal{R}[f](r_-,\varphi)\right).$$

Proof of Theorem 1. In order to facilitate the subsequent proofs, some properties of Fourier transform are introduced primarily. The rules of functional relations of Fourier transform are shown in the **Appendix** [14].

For the target $f(\vec{\boldsymbol{x}})$, on the promise that $f(\vec{\boldsymbol{x}})$ satisfies **Hypothesis 1**, then according to the properties of Fourier transform, there is

$$f(\vec{\boldsymbol{x}})=\mathcal{F}_{\vec{\xi}}^{-1}\left[\mathcal{F}_{\vec{x}}[f]\right](\vec{\boldsymbol{x}})=\iint_{\mathbb{R}^2}\mathcal{F}_{\vec{x}}[f]\left(\vec{\boldsymbol{\xi}}\right)\cdot\exp\left(2\pi\boldsymbol{i}\vec{\boldsymbol{\xi}}^T\vec{\boldsymbol{x}}\right)\mathrm{d}^2\vec{\boldsymbol{\xi}},$$

where, $\mathcal{F}_{\vec{x}}[\otimes]\left(\vec{\boldsymbol{\xi}}\right)$ is the 2-D Fourier transform for independent variables $\vec{\boldsymbol{x}}$; $\vec{\boldsymbol{\xi}}=(\xi,\psi)^T$ are the independent variables in frequency domain corresponding to $\vec{\boldsymbol{x}}$; $\mathcal{F}_{\vec{\xi}}^{-1}[\otimes](\vec{\boldsymbol{x}})$ is the inverse 2-D Fourier transform for independent variables $\vec{\boldsymbol{\xi}}$. Replace variable $\vec{\boldsymbol{\varphi}}\rho\leftarrow\vec{\boldsymbol{\xi}}$, and combined with Jacobian determinant, there is

$$\mathrm{d}^2\vec{\boldsymbol{\xi}}=\begin{vmatrix}\cos\varphi & -\rho\sin\varphi\\ \sin\varphi & \rho\cos\varphi\end{vmatrix}\mathrm{d}\rho\mathrm{d}\varphi=\rho\mathrm{d}\rho\mathrm{d}\varphi.$$

The orthogonal direction integral of rectangular coordinate system is transformed into the rotation direction integral of polar coordinate system. According to the central slice theorem [15], there is

Preprints (www.preprints.org) | NOT PEER-REVIEWED | Posted: 14 January 2022 doi:10.20944/preprints202201.0199.v1

$$f(\vec{\boldsymbol{x}})=\frac{1}{2}\int_0^{2\pi}\int_{\mathbb{R}}\mathcal{F}_r\left[\mathcal{R}[f](r,\varphi)\right](\rho)\cdot\exp\left(2\pi\boldsymbol{i}\rho\vec{\boldsymbol{\varphi}}^T\vec{\boldsymbol{x}}\right)\cdot|\rho|\mathrm{d}\rho\mathrm{d}\varphi\,, \tag{3}$$

where $\mathcal{F}_r[\otimes](\rho)$ is the Fourier transform for variable r. For $|\rho|$ in Equation (3), there is

$$|\rho|=\rho\,\mathrm{sgn}(\rho)=-\boldsymbol{i}\,\mathrm{sgn}(\rho)\cdot\boldsymbol{i}\rho\,,$$

where $\mathrm{sgn}(\bullet)$ represents the Sign function. According to **Rule 6**, there is

$$\delta(r)=\mathcal{F}[1](\rho)=\mathcal{F}_r\left[r\cdot\frac{1}{r}\right](\rho)=\frac{\boldsymbol{i}}{2\pi}\cdot\frac{\mathrm{d}}{\mathrm{d}\rho}\left(\mathcal{F}_r\left[\frac{1}{r}\right](\rho)\right),$$

where $\delta(\bullet)$ represents the Dirac delta function. Combined with the principle of parity invariance,

$$\mathcal{F}_r\left[\frac{1}{r}\right](\rho)=-\pi\boldsymbol{i}\,\mathrm{sgn}(\rho)\,.$$

By inverse Fourier transform, there is

$$\mathcal{F}_\rho^{-1}\left[-\boldsymbol{i}\,\mathrm{sgn}(\rho)\right](r)=\frac{1}{\pi r}, \tag{4}$$

where $\mathcal{F}_\rho^{-1}[\otimes](r)$ is the inverse Fourier transform for variable ρ in frequency domain. According to **Rule 5**, there is

$$\mathcal{F}_\rho^{-1}\left[\boldsymbol{i}\rho\cdot\mathcal{F}_r\left[\mathcal{R}[f](r,\varphi)\right](\rho)\right](r)=\frac{1}{2\pi}\cdot\frac{\partial}{\partial r}\mathcal{R}[f](r,\varphi)\,. \tag{5}$$

By substituting Equation (4) and Equation (5) into Equation (3), and according to **Rule 1** and **Rule 7**, the inverse Radon transform formula in the form of Hilbert transform is obtained, as

$$f(\vec{\boldsymbol{x}})=\frac{1}{4\pi}\int_0^{2\pi}\mathbf{H}_\tau\left[\frac{\partial}{\partial\tau}\mathcal{R}[f](\tau,\varphi)\right](r)\Big|_{r=\vec{\boldsymbol{\varphi}}^T\vec{\boldsymbol{x}}}\mathrm{d}\varphi\,. \tag{6}$$

where $\mathbf{H}_\tau[\otimes](r)$ is the Hilbert transform for variable τ.

In Equation (6), the derivative term in the Hilbert transform makes the radon inverse transform formula very sensitive to the small error in the projections, which is not conducive to accurate reconstruction. Combined with the definition of convolution, the Hilbert transform defined using the Cauchy principal value (marked with **p.v.**) is given by

$$\mathbf{H}_\tau\left[\frac{\partial}{\partial\tau}\mathcal{R}[f](\tau,\varphi)\right](r):=\mathbf{p.v.}\int_{\mathbb{R}}\frac{1}{\pi(r-\tau)}\cdot\frac{\partial}{\partial\tau}\mathcal{R}[f](\tau,\varphi)\mathrm{d}\tau\,. \tag{7}$$

On the basis that the anomalous integral in Equation (7) converges, the right side of Equation (7) can be transformed by the partial integration, as

$$\int\frac{1}{r-\tau}\cdot\frac{\partial}{\partial\tau}\mathcal{R}[f](\tau,\varphi)\mathrm{d}\tau=\frac{\mathcal{R}[f](\tau,\varphi)+C}{r-\tau}-\int\frac{\mathcal{R}[f](\tau,\varphi)+C}{(r-\tau)^2}\mathrm{d}\tau\,. \tag{8}$$

where C is a constant. To ensure the validity of the partial integration, the convergence of the integral on the right side of Equation (8) must be guaranteed, so there is $C=-\mathcal{R}[f](r,\varphi)$. Equation (6) is further equivalent to

$$f(\vec{\boldsymbol{x}})=\frac{1}{4\pi^2}\cdot\mathbf{p.v.}\int_0^{2\pi}\int_{\mathbb{R}}\frac{\mathcal{R}[f](r,\varphi)-\mathcal{R}[f](\tau,\varphi)}{(r-\tau)^2}\Big|_{r=\vec{\boldsymbol{\varphi}}^T\vec{\boldsymbol{x}}}\mathrm{d}\tau\mathrm{d}\varphi\,. \tag{9}$$

Preprints (www.preprints.org) | NOT PEER-REVIEWED | Posted: 14 January 2022 doi:10.20944/preprints202201.0199.v1

Eliminate the singularity of the integrand in Equation (9), then replace variable $s \leftarrow r-\tau$. Equation (2) is obtained, which is the formula of SDBP technique. **Theorem 1** has been proved. □

3. Computational Model for Filter Expressions

On the basis of SDBP technique, we have proposed a filter construction method. Implemented in spatial domain, the method reveals the relationship between the filter function and the convolution kernel, which can be used to restore discrete sampling data into continuous functions by convolution.

3.1. Projection Data Preprocess

For the target $f(\vec{x})$, on the premise that the projection of $f(\vec{x})$ at any angle is systematic sampling data, it is assumed that the known conditions are:

Hypothesis 3.

1. The sampling interval of the detector is d, $d \in \mathbb{R}_+$;
2. The projection angles are discrete at equal intervals, and M is the number of total projections;
3. For $m \in \mathbb{N}$ and $n \in \mathbb{Z}$, the projection value is defined as

$$P_m(n) \coloneqq \int_{\mathbb{R}} \mathcal{R}[f](r,\varphi_m) \cdot \delta(r-nd)\,\mathrm{d}r,$$

where $\varphi_m = 2\pi m/M$.

In order to acquire the continuous second-order difference projection function at any angle whose domain is $\mathbb{R}$, the discrete projection signal should be converted into a continuous function. Construct the continuous second-order difference projection function $\Delta_n^2\left[\tilde{P}_m\right](\hat{s})$ of $\hat{s} \in \mathbb{R}$ via projection values $P_m(n)$, where $\hat{s}$ is the normalized variable of s as $\hat{s} = s/d$. The constructed $\Delta_n^2\left[\tilde{P}_m\right](\hat{s})$ is expressed as:

Definition 2. For $m \in \mathbb{N}$, $n \in \mathbb{Z}$, $\nu \in \mathbb{Z}$, $\hat{s} \in \mathbb{R}$,

$$\Delta_n^2\left[\tilde{P}_m\right](\hat{s}) \coloneqq \sum_{\nu \in \mathbb{Z}} \left(\Delta_n^2[P_m](\nu) \cdot k(\hat{s}-\nu)\right). \tag{10}$$

where $k(\bullet)$ represents the convolution kernel function, and $k(\hat{s})$ of $\hat{s} \in \mathbb{R}$ satisfies the following conditions:

Hypothesis 4. For $\nu \in \mathbb{Z}$, $\hat{s} \in \mathbb{R}$,

1. $k(\hat{s})$ is piecewise continuous, and the integral $\int_{\mathbb{R}} k(\hat{s})\mathrm{d}\hat{s} = 1$;
2. $k(\hat{s}) = k(-\hat{s})$, $k(\nu)\big|_{\nu \neq 0} = 0$, and $\lim\limits_{t \to \infty} k(\hat{s}) = 0$;
3. $k(\hat{s})$ is differentiable at any $\hat{s} = \nu \neq 0$;
4. The second derivative $\dfrac{\mathrm{d}^2 k(\hat{s})}{\mathrm{d}\hat{s}^2}$ is continuous in the deleted neighbourhood of any $\hat{s} = \nu \neq 0$, and $\dfrac{\mathrm{d}^2 k(\hat{s})}{\mathrm{d}\hat{s}^2}$ converges on both sides of any $\hat{s} = \nu \neq 0$.

3.2. Conversion relation between convolution kernels and filter functions

The reconstructed value $f(\vec{x})$ of $\vec{x} \in \mathbb{R}^2$ can be approximated by

Preprints (www.preprints.org) | NOT PEER-REVIEWED | Posted: 14 January 2022 doi:10.20944/preprints202201.0199.v1

$$\hat{f}(\vec{x}) = \frac{\pi d}{M} \sum_{m=0}^{M-1} \sum_{n \in \mathbb{Z}} \left(P_m \left(\left\lfloor \vec{\varphi}_m^T \vec{x} / d + 1/2 \right\rfloor - n \right) \cdot h(n) \right), \tag{11}$$

where, $\vec{\varphi}_m = (\cos\varphi_m, \sin\varphi_m)^T$; $\lfloor \bullet \rfloor$ represents the floor function, which gives the largest integer no greater than the input real number; $h(n)$ is the amplitude sequence of CT reconstruction filter, which can be obtained by $k(\hat{s})$ as follows:

Theorem 2. For $n \in \mathbb{Z} \setminus \{0\}$, $\tau \in \mathbb{R}$, there is

$$h(n)\big|_{n \neq 0} = \frac{1}{2\pi d^2} \mathbf{H}_\tau \left[\frac{\mathrm{d}k(\tau)}{\mathrm{d}\tau} \right](n); \tag{12}$$

if $n = 0$, there is

$$h(0) = -\sum_{n \in \mathbb{Z}} h(n)\big|_{n \neq 0}. \tag{13}$$

For any given kernel function, its corresponding filter is uniquely determined. On the other hand, the kernel function corresponding to any given $h(n)$ is not unique.

Given the analytic function (not unique) of $h(n)\big|_{n \neq 0}$, which is $h(\hat{r})$ of $\hat{r} \in \mathbb{R}$, where $\hat{r}$ is the normalized variable of r as $\hat{r} = r/d$, the corresponding convolution kernel of $h(\hat{r})$ is as follows:

Theorem 3. For $\hat{s} \in \mathbb{R}$, $\tau \in \mathbb{R}$, there is

$$k(\hat{s}) = 2\pi d^2 \mathbf{H}_\tau \left[\int h(\tau) \mathrm{d}\tau \right](\hat{s}). \tag{14}$$

By applying the above computational model of filters, a variety of new filters can be obtained by designing the interpolation functions. Conversely, according to Equation (14), the kernel functions corresponding to some commonly used filters have been revealed. Therefore, the form of CT reconstruction filter is closely related to the restoration process of projection signal.

Proof of Theorem 2. For the discrete projections, according to the SDBP technique, the inverse transform can be approximately expressed as

$$f(\vec{x}) \approx -\frac{1}{2\pi M} \lim_{\varepsilon \to 0+} \sum_{m=0}^{M-1} \int_\varepsilon^{+\infty} \frac{\Delta_r^2 \left[\mathcal{R}[f](r, \varphi_m) \right](s)}{s^2} \bigg|_{r = \vec{\varphi}_m^T \vec{x}} \mathrm{d}s.$$

Replace variable $\hat{s} \leftarrow s/d$, then replace the second-order difference with $\Delta_n^2 \left[\tilde{P}_m \right](\hat{s})$ in Equation (10). The estimation formula of reconstructed $f(\vec{x})$ can be acquired, as

$$\tilde{f}(\vec{x}) = -\frac{1}{2\pi d M} \lim_{\varepsilon \to 0+} \sum_{m=0}^{M-1} \int_\varepsilon^{+\infty} \frac{\Delta_n^2 \left[\tilde{P}_m \right](\hat{s})}{\hat{s}^2} \bigg|_{n = \left\lfloor \frac{\vec{\varphi}_m^T \vec{x}}{d} + \frac{1}{2} \right\rfloor} \mathrm{d}\hat{s}, \tag{15}$$

According to Equation (10), Equation (15) can be further transformed into

Preprints (www.preprints.org) | NOT PEER-REVIEWED | Posted: 14 January 2022 doi:10.20944/preprints202201.0199.v1

$$\tilde{f}(\vec{x}) = -\frac{1}{2\pi dM}\lim_{\varepsilon\to 0+}\sum_{m=0}^{M-1}\sum_{\nu\in\mathbb{N}_+}\left(\Delta_n^2[P_m](\nu)\cdot\mathbf{p.v.}\int_{\mathbb{R}}\frac{k(\nu-\tau)}{\tau^2}\mathrm{d}\tau\right)\Bigg|_{n=\left\lfloor\frac{\vec{\varphi}_m^T\vec{x}}{d}+\frac{1}{2}\right\rfloor}. \tag{16}$$

In the light of the operational characteristics of discrete convolution, Equation (16) can be transformed into Equation (11), in which

$$h(n)\big|_{n\neq 0} = -\frac{1}{2\pi^2 d^2}\cdot\mathbf{p.v.}\int_{\mathbb{R}}\frac{k(n-\tau)}{\tau^2}\mathrm{d}\tau. \tag{17}$$

By performing partial integral in Equation (17), there is

$$h(n)\big|_{n\neq 0} = \frac{1}{2\pi d^2}\cdot\mathbf{p.v.}\int_{\mathbb{R}}\frac{1}{\pi\tau}\cdot\frac{\mathrm{d}k(n-\tau)}{\mathrm{d}\tau}\mathrm{d}\tau.$$

Combined with the definition of Hilbert transform, Equation (12) can be acquired. Since the sum of all the $P_m(n)$ coefficients in Equation (16) is zero, Equation (13) holds, therefore **Theorem 2** has been proved. □

Proof of Theorem 3. Inversely, if the analytic function $h(\hat{s})$ of $\hat{s}\in\mathbb{R}$ is given, then $h(\hat{s})$ satisfies Equation (17), as

$$h(\hat{s}) = -\frac{1}{2\pi^2 d^2}\cdot\mathbf{p.v.}\int_{\mathbb{R}}\frac{k(\hat{s}-\tau)}{\tau^2}\mathrm{d}\tau.$$

By Fourier transform and according to **Rule 7**, there is

$$\mathcal{F}_\tau[h](\hat{\rho}) = -\frac{1}{2\pi^2 d^2}\cdot\mathcal{F}_\tau[k](\hat{\rho})\cdot\mathcal{F}_\tau\left[\frac{1}{\tau^2}\right](\hat{\rho}). \tag{18}$$

For $\mathcal{F}_\tau\left[\frac{1}{\tau^2}\right](\hat{\rho})$, according to **Rule 5**, there is

$$\mathcal{F}_\tau\left[\frac{1}{\tau^2}\right](\hat{\rho}) = \mathcal{F}_\tau\left[-\frac{\mathrm{d}}{\mathrm{d}\tau}\left(\frac{1}{\tau}\right)\right](\hat{\rho}) = -2\pi\boldsymbol{i}\hat{\rho}\cdot\mathcal{F}_\tau\left[\frac{1}{\tau}\right](\hat{\rho}) = -2\pi^2|\hat{\rho}|. \tag{19}$$

By substituting Equation (19) into Equation (18), the following equation is acquired after performing inverse Fourier transform, as

$$k(\hat{s}) = d^2\mathcal{F}_{\hat{\rho}}^{-1}\left(\frac{\mathcal{F}_\tau[h](\hat{\rho})}{|\hat{\rho}|}\right)(\hat{s}). \tag{20}$$

In Equation (20), there is

$$\frac{\mathcal{F}_\tau[h](\hat{\rho})}{|\hat{\rho}|} = -2\pi\boldsymbol{i}\,\mathrm{sgn}(\hat{\rho})\cdot\frac{\mathcal{F}_\tau[h](\hat{\rho})}{2\pi\boldsymbol{i}\hat{\rho}}. \tag{21}$$

According to **Rule 5**,

$$\mathcal{F}_\tau[h](\hat{\rho}) = 2\pi\boldsymbol{i}\hat{\rho}\cdot\mathcal{F}_\tau\left[\int h(\tau)\mathrm{d}\tau\right](\hat{\rho}). \tag{22}$$

By substituting Equation (22) into Equation (21), it can be deducted that

$$\frac{\mathcal{F}_\tau[h](\hat{\rho})}{|\hat{\rho}|} = -2\pi\boldsymbol{i}\,\mathrm{sgn}(\hat{\rho})\cdot\mathcal{F}_\tau\left[\int h(\tau)\mathrm{d}\tau\right](\hat{\rho}). \tag{23}$$

According to **Rule 7** and combined with Equation (4), the following equation is acquired after performing Fourier transform on both sides of Equation (23), as

Preprints (www.preprints.org) | NOT PEER-REVIEWED | Posted: 14 January 2022 doi:10.20944/preprints202201.0199.v1

$$\mathcal{F}_{\hat{\rho}}^{-1}\left(\frac{\mathcal{F}_{\tau}[h](\hat{\rho})}{|\hat{\rho}|}\right)(\hat{s})=2\pi\cdot\mathbf{p.v.}\int_{\mathbb{R}}\frac{\int h(\tau)\mathrm{d}\tau}{\pi(\hat{s}-\tau)}\mathrm{d}\tau\,. \tag{24}$$

By substituting Equation (24) into Equation (20), and combined with the definition of Hilbert transform, Equation (14) can be acquired. **Theorem 3** has been proved. □

It can be clearly observed that there is a reciprocal relationship between filter function $h(\bullet)$ and kernel function $k(\bullet)$, which can be realized by Hilbert transform, shown as follows:

$$h(\bullet)\underset{\frac{1}{2\pi d^2}\mathbf{H}_{\tau}\left[\frac{\mathrm{d}k(\tau)}{\mathrm{d}\tau}\right](\bullet)}{\overset{2\pi d^2\mathbf{H}_{\tau}\left[\int h(\tau)\mathrm{d}\tau\right](\bullet)}{\rightleftarrows}}k(\bullet)\,.$$

Based on the principles above, the mutual conversion between filter function and kernel function can be realized. It shows the correlation between the filter design and data restoration.

4. Illustration with Examples

To verify the validity of the proposed method of constructing filters, we have applied some common kernels to the proposed model as examples, by which some known filters have been derived. We also compared the reconstruction errors of different filters.

4.1. R-L filter: $\mathrm{sinc}(\bullet)$ *kernel*

If $\Delta_n^2\left[\tilde{P}_m\right](\hat{s})$ of $\hat{s}\in\mathbb{R}$ is the Whittaker-Shannon interpolation of $\Delta_n^2\left[P_m\right](\nu)$, then the convolution kernel is the normalized sinc function, as

$$k(\hat{s})=\mathrm{sinc}(\pi\hat{s})\,.$$

The derivative of normalized sinc function is

$$\frac{\mathrm{d}}{\mathrm{d}\tau}\mathrm{sinc}(\pi\tau)=\frac{\tau\cos(\pi\tau)-\sin(\pi\tau)}{\pi\tau^2}\,.$$

According to Equation (12), there is

$$h_{\mathrm{sinc}}(n)\big|_{n\neq 0}=\frac{1}{2\pi d^2}\cdot\mathbf{p.v.}\int_{\mathbb{R}}\frac{\tau\cos(\pi\tau)-\sin(\pi\tau)}{\pi^2\tau^2(n-\tau)}\mathrm{d}\tau=-\frac{1-(-1)^n}{2\pi^2n^2d^2}\,.$$

By Equation (13),

$$h_{\mathrm{sinc}}(0)=-\frac{1}{\pi^2d^2}\sum_{n\in\mathbb{N}_+}\frac{(-1)^n-1}{n^2}=\frac{3\varsigma(2)}{2\pi^2d^2}=\frac{1}{4d^2}\,.$$

where $\varsigma(\bullet)$ represents the Riemann zeta function, and $\varsigma(2)=\frac{\pi^2}{6}$. Therefore, the filter corresponding to normalized sinc kernel is

$$h_{\mathrm{sinc}}(n)=\begin{cases}\dfrac{1}{4d^2}, & n=0\\ -\dfrac{1-(-1)^n}{2\pi^2n^2d^2}, & n\neq 0\end{cases}\,. \tag{25}$$

Equation (25) is the expression of R-L filter [8].

4.2. S-L filter: $\Pi(\bullet)$ *kernel*

Preprints (www.preprints.org) | NOT PEER-REVIEWED | Posted: 14 January 2022 doi:10.20944/preprints202201.0199.v1

If $\Delta_n^2\left[\tilde{P}_m\right](\hat{s})$ of $\hat{s}\in\mathbb{R}$ is the proximal interpolation of $\Delta_n^2\left[P_m\right](\nu)$, then the kernel function is the unit rectangular function, as

$$k(\hat{s})=\Pi(\hat{s}),$$

where $\Pi(\bullet)$ represents the unit rectangular function. The generalized derivative of unit rectangular function is

$$\frac{\mathrm{d}}{\mathrm{d}\tau}\Pi(\tau):=\delta(\tau+1/2)-\delta(\tau-1/2).$$

According to Equation (12), there is

$$h_{\Pi}(n)\big|_{n\neq 0}=\frac{1}{2\pi d^2}\int_{\mathbb{R}}\frac{\delta(\tau+1/2)-\delta(\tau-1/2)}{\pi(n-\tau)}\mathrm{d}\tau=-\frac{2}{\pi^2d^2\left(4n^2-1\right)}.$$

By Equation (13),

$$h_{\Pi}(0)=\frac{4}{\pi^2d^2}\sum_{n\in\mathbb{N}_+}\frac{1}{4n^2-1}=\frac{2}{\pi^2d^2}.$$

Therefore, the filter corresponding to unit rectangular kernel is

$$h_{\Pi}(n)=\begin{cases}\dfrac{2}{\pi^2d^2}, & n=0\\ -\dfrac{2}{\pi^2d^2\left(4n^2-1\right)}, & n\neq 0\end{cases}. \tag{26}$$

Equation (26) is the expression of S-L filter [9].

4.3. Delta filter: $\delta(\bullet)$ kernel

If $\Delta_n^2\left[\tilde{P}_m\right](\hat{s})$ of $\hat{s}\in\mathbb{R}$ is the sampling function with each amplitude $\Delta_n^2\left[P_m\right](\nu)$, then the convolution kernel is the unit delta function, as

$$k(\hat{s})=\delta(\hat{s}).$$

According to Equation (12), there is

$$h_{\delta}(n)\big|_{n\neq 0}=\frac{1}{2\pi d^2}\int_{\mathbb{R}}\frac{\mathrm{d}\delta(\tau)}{\mathrm{d}\tau}\cdot\frac{1}{\pi(n-\tau)}\mathrm{d}\tau=-\frac{1}{2\pi d^2}\int_{\mathbb{R}}\frac{\delta(\tau)}{\pi(n-\tau)^2}\mathrm{d}\tau=-\frac{1}{2\pi^2n^2d^2}.$$

By Equation (13),

$$h_{\delta}(0)=\frac{1}{\pi^2d^2}\sum_{n\in\mathbb{N}_+}\frac{1}{n^2}=\frac{\varsigma(2)}{\pi^2d^2}=\frac{1}{6d^2}.$$

Therefore, the filter corresponding to unit delta kernel is

$$h_{\delta}(n)=\begin{cases}\dfrac{1}{6d^2}, & n=0\\ -\dfrac{1}{2\pi^2n^2d^2}, & n\neq 0\end{cases}. \tag{27}$$

The expression of delta filter shown in Equation (27) was firstly proposed by Yuchuan Wei and Ge Wang [16], which was introduced as a practical filter to approximate the ideal filter.

4.4. Imaging tests

Preprints (www.preprints.org) | NOT PEER-REVIEWED | Posted: 14 January 2022 doi:10.20944/preprints202201.0199.v1

The Shepp-Logan phantom of 1024×1024 pixels was used to test CT imaging performance of different example filters. The number of projections was set to 720, and the sampling interval of the detector was equal to the pixel size of the phantom. For further comparison, Gaussian white noise of standard deviation σ was added to the sinogram to test the performance of the filters in noise. The reconstructed images are shown in **Figure 1**.

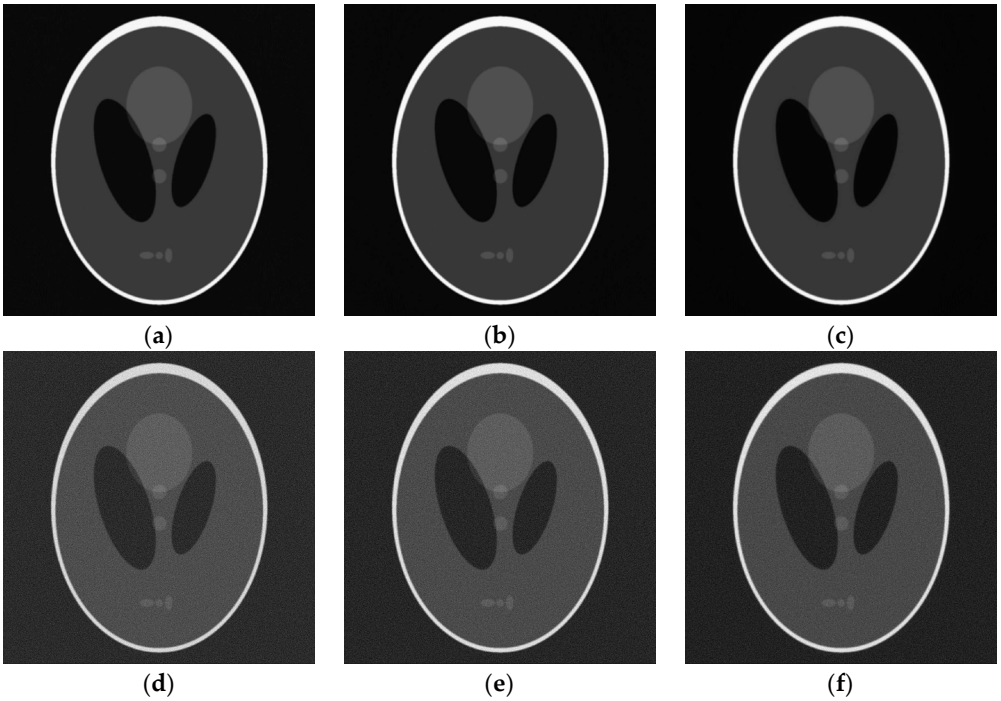

Figure 1. Reconstructed Shepp-Logan phantom images by exemplified filters: (a) R-L filter without noise; (b) S-L filter without noise; (c) Delta filter without noise; (d) R-L filter in noise of $\sigma = 5$; (e) S-L filter in noise of $\sigma = 5$; (f) Delta filter in noise of $\sigma = 5$.

To reflect the reconstruction accuracy more intuitively, we used the root mean square error (RMSE) to evaluate the error between the reconstructed image and the original image. The RMSE of CT image is defined as follows:

$$\mathrm{RMSE} = \sqrt{\frac{\sum_{u=1}^{N}\sum_{v=1}^{N}\left(\tilde{f}_{u,v} - f_{u,v}\right)^2}{\sum_{u=1}^{N}\sum_{v=1}^{N} f_{u,v}^2}},$$

where, $f_{u,v}$ is the gray value of the original image pixel in row u and column v; $\tilde{f}_{u,v}$ is the gray value of the reconstructed image pixel in row u and column v; N is the maximum value of u and column v. By calculation, the RMSE table of reconstructed images is shown in **Table 1**, which shows that the reconstructed image of delta filter has the smallest RMSE under each noise intensity.

Table 1. RMSE of reconstructed images.

Noise Density	R-L Filter	S-L Filter	Delta Filter
$\sigma = 0$	0.2672	0.2508	0.2431
$\sigma = 1$	0.3231	0.2919	0.2784
$\sigma = 5$	0.6544	0.5886	0.5332

5. Analysis of Basic Composition of Filters

Preprints (www.preprints.org) | NOT PEER-REVIEWED | Posted: 14 January 2022 doi:10.20944/preprints202201.0199.v1

In order to make further explorations in the rules of the filter properties changing with the kernels, we have discussed the basic components of CT reconstruction filters, that the amplitude sequence of any filter can be decomposed into a linear combination of those of basic filters, similar to Fourier transform. The properties of basic filters provide guidance for the design of kernel functions.

5.1 Decomposition of kernel functions

A generalized function can be described by Schwartz-distribution. As for the kernel function $k(\bullet)$, its Schwartz-distribution is defined by

$$\langle k, \mathfrak{T} \rangle := \int_{\mathbb{R}} k(\tau) \cdot \mathfrak{T}(\tau) \mathrm{d}\tau, \tag{28}$$

where $\mathfrak{T}(\bullet)$ represents the test function.

By performing discretization, the local function in a definite interval is regarded as a delta function whose amplitude is equal to the interval integral. In this way, the kernel function can be decomposed to a combination of delta functions. Assume that the interval between any adjacent integers is equally divided by piecewise intervals, then the discretized kernel function can be defined as follows:

Definition 3. For $\nu \in \mathbb{Z}$, $\Lambda \in \mathbb{N}_+$, $\tau \in \mathbb{R}$,

$$\tilde{k}_\Lambda(\tau) := \sum_{\nu \in \mathbb{Z}} \left(\delta\left(\tau - \frac{2\nu+1}{2\Lambda}\right) \cdot \int_{\mathbb{R}} k(\tau) \cdot \Pi\left(\Lambda\tau - \frac{2\nu+1}{2}\right) \mathrm{d}\tau \right). \tag{29}$$

Considering when $\Lambda \to \infty$, by applying Equation (28) to Equation (29), there is

$$\left\langle \tilde{k}_\Lambda, \mathfrak{T} \right\rangle\Big|_{\Lambda\to\infty} = \lim_{\Lambda\to\infty} \sum_{\nu \in \mathbb{Z}} \left(\mathfrak{T}\left(\frac{2\nu+1}{2\Lambda}\right) \cdot \int_{\mathbb{R}} k(\tau) \cdot \Pi\left(\Lambda\tau - \frac{2\nu+1}{2}\right) \mathrm{d}\tau \right).$$

If $\mathfrak{T}(\bullet)$ is continuous within its domain, according to the first mean value theorem for definite integrals, the discretized kernel $\tilde{k}_\Lambda(\bullet)$ when $\Lambda \to \infty$ and the original kernel $k(\bullet)$ have the identical Schwartz-distribution,

$$\left\langle \tilde{k}_\Lambda, \mathfrak{T} \right\rangle\Big|_{\Lambda\to\infty} = \lim_{\Lambda\to\infty} \sum_{\nu \in \mathbb{Z}} \left(\int_{\mathbb{R}} k(\tau) \cdot \mathfrak{T}(\tau) \cdot \Pi\left(\Lambda\tau - \frac{2\nu+1}{2}\right) \mathrm{d}\tau \right) = \langle k, \mathfrak{T} \rangle. \tag{30}$$

To describe the basic elements of kernel functions, the delta_2 function $\delta_2(\bullet, \lambda)$ has been defined, which is described as:

Definition 4. For $\lambda \in \mathbb{R}$, $\tau \in \mathbb{R}$,

$$\delta_2(\tau, \lambda) := \frac{1}{2}\left(\delta(\tau - \lambda) + \delta(\tau + \lambda)\right), \tag{31}$$

where λ represents the displacement of the delta functions from the origin.

According to the conditions in **Hypothesis 4**, $\tilde{k}_\Lambda(\tau)$ can be expressed in the following form, as

$$\tilde{k}_\Lambda(\tau) = \sum_{\nu \in \mathbb{Z}} \left(\mathfrak{a}_\Lambda(\nu) \cdot \delta_2\left(\tau, \frac{2\nu+1}{2\Lambda}\right) \right), \tag{32}$$

where $\mathfrak{a}_\Lambda(\nu)$ is the amplitude of delta_2 function,

Preprints (www.preprints.org) | NOT PEER-REVIEWED | Posted: 14 January 2022 doi:10.20944/preprints202201.0199.v1

$$\mathfrak{a}_\Lambda(\nu)=\int_{\mathbb{R}}k(\tau)\cdot\Pi\left(\Lambda\tau-\frac{2\nu+1}{2}\right)\mathrm{d}\tau\,.$$

According to **Hypothesis 4**, $\mathfrak{a}(\nu)$ satisfies:

1. $\sum_{\nu\in\mathbb{Z}}\mathfrak{a}_\Lambda(\nu)=1$;
2. $\mathfrak{a}_\Lambda(\nu)=\mathfrak{a}_\Lambda(-\nu)$;
3. For a finite fixed value of Λ, $\lim_{\nu\to\infty}\mathfrak{a}_\Lambda(\nu)=0$.

5.2 Filters of Basic Type

In the definition of Schwartz-distribution, the delta_2 function is the basis function of any kernel. According to Equation (12) and Equation (31), if $\delta_2(\tau,\lambda)$ is the kernel function of $\tau\in\mathbb{R}$ and $\lambda\in\mathbb{R}\setminus\mathbb{Z}$, there is

$$h_{\delta_2}(n,\lambda)\big|_{n\neq0}=-\frac{1}{4\pi d^2}\int_{\mathbb{R}}\frac{\delta(\tau-\lambda)+\delta(\tau+\lambda)}{\pi(n-\tau)^2}\mathrm{d}\tau=-\frac{1}{4\pi^2d^2}\left(\frac{1}{(n-\lambda)^2}+\frac{1}{(n+\lambda)^2}\right).\quad(33)$$

By Equation (13), the following equation can be acquired,

$$h_{\delta_2}(0,\lambda)=-\frac{1}{2\pi^2\lambda^2d^2}-\frac{1}{2\pi^2d^2}\cdot\left(\frac{\mathrm{d}}{\mathrm{d}\tau}\sum_{n\in\mathbb{Z}}\left(\frac{1}{n+\tau}\right)\right)\Big|_{\tau=\lambda}.\quad(34)$$

The partial fraction decomposition of cotangent function is used to calculate the exact value of $h(0)$: For $\tau\in\mathbb{R}\setminus\mathbb{Z}$, the sum of the sequence in Equation (34) is

$$\sum_{n\in\mathbb{Z}}\frac{1}{n+\tau}=\pi\cot(\pi\tau)\,.$$

Therefore,

$$h_{\delta_2}(0,\lambda)=\frac{1}{2d^2}\left(\frac{1}{\sin^2(\pi\lambda)}-\frac{1}{\pi^2\lambda^2}\right).\quad(35)$$

Combined with Equation (33) and Equation (35), the filter corresponding to delta_2 function kernel is

$$h_{\delta_2}(n,\lambda)=\begin{cases}\dfrac{1}{2d^2}\left(\dfrac{1}{\sin^2(\pi\lambda)}-\dfrac{1}{\pi^2\lambda^2}\right), & n=0\\[2ex] -\dfrac{1}{4\pi^2d^2}\left(\dfrac{1}{(n-\lambda)^2}+\dfrac{1}{(n+\lambda)^2}\right), & n\neq0\end{cases}.\quad(36)$$

Equation (36) is the expression of basic filter series. The operation in Equation (12) satisfies the expression of Schwartz-distribution in Equation (28). Combined with Equation (30), it can be concluded that $\tilde{k}_\Lambda(\bullet)$ and $k(\bullet)$ correspond to the same filter when $\Lambda\to\infty$, which means

$$\lim_{\Lambda\to\infty}\tilde{h}_\Lambda(n)=h(n)\,.$$

where $\tilde{h}_\Lambda(n)$ corresponds to $\tilde{k}_\Lambda(\tau)$. On the basis of the linearity in Equation (12), it can be derived from Equation (32) that

$$\tilde{h}_\Lambda(n)=\sum_{\nu\in\mathbb{Z}}\left(\mathfrak{a}_\Lambda(\nu)\cdot h_{\delta_2}\left(n,\frac{2\nu+1}{2\Lambda}\right)\right).\quad(37)$$

Preprints (www.preprints.org) | NOT PEER-REVIEWED | Posted: 14 January 2022 doi:10.20944/preprints202201.0199.v1

If $k(\tau)$ is continuous for $\tau \in \left(\frac{\nu}{\Lambda}, \frac{\nu+1}{\Lambda}\right)$, then

$$\lim_{\Lambda\to\infty} \mathfrak{a}_{\Lambda}(\nu) = \lim_{\Lambda\to\infty}\left(\frac{1}{\Lambda}\cdot k\left(\frac{2\nu+1}{2\Lambda}\right)\right). \tag{38}$$

Suppose that $k(\tau)$ is continuous for $\tau \in \mathbb{R}$. According to Equation (37) and Equation (38), there is

$$\lim_{\Lambda\to\infty} \tilde{h}_{\Lambda}(n) = \lim_{\Lambda\to\infty}\sum_{\nu\in\mathbb{Z}}\left(\frac{1}{\Lambda}\cdot k\left(\frac{2\nu+1}{2\Lambda}\right)\cdot h_{\delta_2}\left(n, \frac{2\nu+1}{2\Lambda}\right)\right). \tag{39}$$

By means of the definition of integral, it can be obtained by the conversion of Equation (39) that the filter acquired by $k(\bullet)$ satisfies

$$h(n) = \int_{\mathbb{R}} k(\lambda)\cdot h_{\delta_2}(n,\lambda)\,\mathrm{d}\lambda. \tag{40}$$

Under the constraint of **Hypothesis 4**, it can be proved that Equation (40) is still valid in the case the kernel function containing finite discontinuities, which include delta function components.

5.3 Imaging tests

The Shepp-Logan phantom of 1024×1024 pixels was used to test CT imaging performance of different basic filters. The number of projections was set to 720, and the sampling interval of the detector was equal to the pixel size of the phantom. The images of Shepp-Logan phantom were reconstructed by a number of basic filters with different λ, and some results are shown in **Figure 2**.

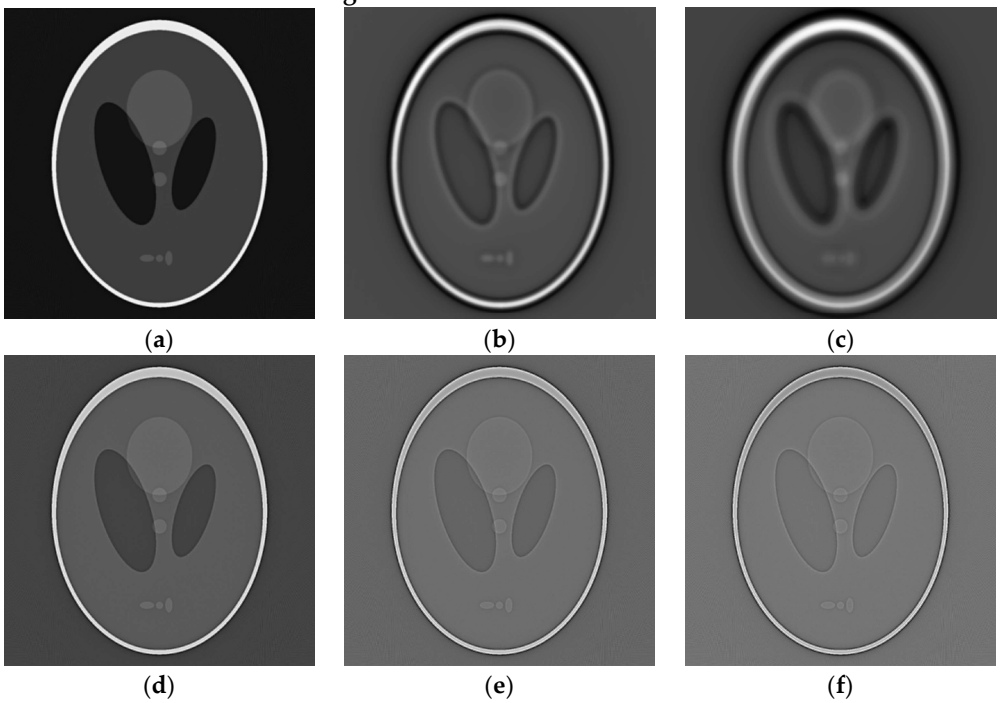

Figure 2. Reconstructed Shepp-Logan phantom images by basic filters of different parameters: (a) $\lambda = 1/2$; (b) $\lambda = 25/2$; (c) $\lambda = 49/2$; (d) $\lambda = 3/4$; (e) $\lambda = 7/8$; (f) $\lambda = 15/16$.

In addition to RMSE, we used the average gradient module (AGM) to measure the sharpness of the CT images. The image sharpness has a positively correlation with AGM. The computing formula of CT image AGM is as follows,

Preprints (www.preprints.org) | NOT PEER-REVIEWED | Posted: 14 January 2022 doi:10.20944/preprints202201.0199.v1

$$\mathrm{AGM}=\frac{\sum_{u=1}^{N}\sum_{v=1}^{N-1}\left|\tilde{f}_{u,v}-\tilde{f}_{u,v+1}\right|+\sum_{u=1}^{N-1}\sum_{v=1}^{N}\left|\tilde{f}_{u,v}-\tilde{f}_{u+1,v}\right|}{2N(N-1)}.$$

The calculated RMSE and AGM of CT images reconstructed by basic filters are shown in **Figure 3** and **Figure 4**.

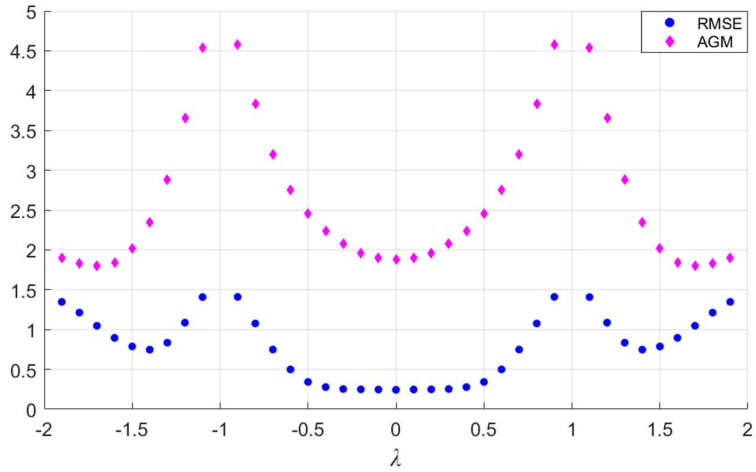

Figure 3. RMSE and AGM of CT images reconstructed by basic filters with different λ ($\lambda=\nu/10$, $\nu\in\mathbb{Z}$ and $\lambda\notin\mathbb{Z}\setminus\{0\}$).

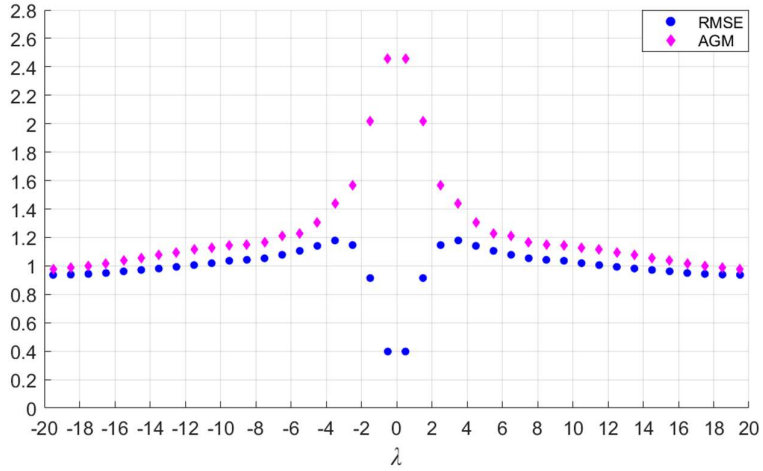

Figure 4. RMSE and AGM of CT images reconstructed by basic filters with different λ ($\lambda=1/2+\nu$ and $\nu\in\mathbb{Z}$).

If the parameter λ is divided into two parts: integer and decimal, as $\lambda=\lambda_0+\lambda_1$ ($\lambda_0\in\mathbb{Z}$ and $\lambda_1\in(-1/2,1/2]$), it can be summarized from **Figure 3** and **Figure 4** that the reconstructed image gradually blurs with the increase of λ_0 while λ_1 is constant, and the sharpness of the image increases as λ_1 is closer to 0 while λ_0 is constant. The RMSE is minimum only when $\lambda=0$. The phenomenon has verified that the delta filter has the characteristic of minimum reconstruction error.

 doi:10.20944/preprints202201.0199.v1

6. Discussion

The SDBP technique proposed in this paper is a method for accurate inverse Radon transform. SDBP is more practicable and more valid than that in the form of Hilbert transform. The transform between the filter function and the kernel function has been derived from the framework of SDBP, which provides a systematic filter design method, that the form and properties of CT reconstruction filter are determined by the convolution kernel in data preprocessing. By extension, a decomposition mode of filters has been proposed. Therefore, filters that meet certain optimal performance indicators can be constructed by referring to the properties of basic filters.

The kernel mentioned in this paper is basically used for projection data restoration. Meanwhile, the kernel is the inverse Fourier transform of the filtering window function in frequency domain. In that sense, the proposed method indicates that the applicable window function has more possibilities, even that the window function does not necessarily have to converge. It shows from a side view that the traditional filter design method does have some limitations.

As a conclusion, any CT reconstruction filter can be decomposed into a linear combination of basic filters. In other words, any CT image reconstructed via FBP is a linear superposition of the images reconstructed by basic filters. However, there are more properties of basic filters need to be revealed. Also, the optimal combination method of basic filters is a subject remains to be studied.

Author Contributions: Conceptualization, Yi-ming Jiang; methodology, Yi-ming Jiang; validation, Yi-ming Jiang and Jing Zou; formal analysis, Yi-ming Jiang; data curation, Jin-tao Zhao; writing—original draft preparation, Yi-ming Jiang; writing—review and editing, Jing Zou; supervision, Xiao-dong Hu; project administration, Xiao-dong Hu; funding acquisition, Jing Zou. All authors have read and agreed to the published version of the manuscript.

Funding: This research was funded by the General Program of National Natural Science Foundation of China (grant number 61771328) and the National Key Research and Development Program of China (grant number 2017YFB1103900).

Data Availability Statement: Not applicable

Conflicts of Interest: The authors declare no conflict of interest. The funders had no role in the design of the study; in the collection, analyses, or interpretation of data; in the writing of the manuscript, or in the decision to publish the results.

Preprints (www.preprints.org) | NOT PEER-REVIEWED | Posted: 14 January 2022 doi:10.20944/preprints202201.0199.v1

Appendix. Table of some functional Fourier transform pairs

Rule Number	Function	Fourier Transform
0	$f(x)$	$\mathcal{F}_x[f](\xi)=\int_{\mathbb{R}} f(x)\cdot\exp(-2\pi \boldsymbol{i}\xi x)\,\mathrm{d}x$
1	$a\cdot f(x)+b\cdot g(x)$	$a\cdot\mathcal{F}_x[f](\xi)+b\cdot\mathcal{F}_x[g](\xi)$
2	$f(x-a)$	$\mathcal{F}_x[f](\xi)\cdot\exp(-2\pi \boldsymbol{i}a\xi)$
3	$f(ax)$	$\frac{1}{\lvert a\rvert}\cdot\mathcal{F}_x[f]\left(\frac{\xi}{a}\right)$
4	$\mathcal{F}_\xi[f](x)$	$f(-\xi)$
5	$\frac{\mathrm{d}^n}{\mathrm{d}x^n}f(x)$	$(2\pi \boldsymbol{i}\xi)^n\cdot\mathcal{F}_x[f](\xi)$
6	$x^n\cdot f(x)$	$\left(\frac{\boldsymbol{i}}{2\pi}\right)^n\cdot\frac{\mathrm{d}^n}{\mathrm{d}\xi^n}\mathcal{F}_x[f](\xi)$
7	$\{f*g\}(x)$	$\mathcal{F}_x[f](\xi)\cdot\mathcal{F}_x[g](\xi)$
8	$f(x)\cdot g(x)$	$\{\mathcal{F}_x[f]*\mathcal{F}_x[g]\}(\xi)$

References

1. Buynak C F, Bossi R H. Applied X-ray computed tomography. *Nuclear Instruments and Methods in Physics Research Section B: Beam Interactions with Materials and Atoms*, **1995**, *99*(*1-4*), 772-774.
2. Plessis A D, Roux S, Guelpa A. Comparison of medical and industrial X-ray computed tomography for non-destructive testing. *Case Studies in Nondestructive Testing & Evaluation*, **2016**, *6*, 17-25.
3. Radon J. On the determination of functions from their integral values along certain manifolds. *IEEE transactions on medical imaging*, **1986**, *5*(*4*), 170-176.
4. Wang C, Zhang H, Zeng Z, et al. Application of Image Reconstruction Based on Inverse Radon Transform in CT System Parameter Calibration and Imaging. *Complexity*, **2021**, *2021*, 1-10.
5. Park H S, Lee S M, Kim H P, et al. CT sinogram consistency learning for metal induced beam hardening correction. *Medical physics*, **2018**, *45*(*12*), 5376-5384.
6. Hongliang H, Weiyu T, Juntao Y, et al. Parameters Calibration of CT System Based On Geometric Model and Inverse Radon Transform. In Proceedings of the *2021 10th International Conference on Applied Science, Engineering and Technology* (*ICASET 2021*). Atlantis Press: Qingdao, China, 2021.
7. Willemink M J, Noël P B. The evolution of image reconstruction for CT—from filtered back projection to artificial intelligence. *European radiology*, **2019**, *29*(*5*), 2185-2195.
8. Ramachandran G N, Lakshminarayanan A V. Three-dimensional Reconstruction from Radiographs and Electron Micrographs: Application of Convolutions instead of Fourier Transforms. *Proceedings of the National Academy of Sciences of the United States of America*, **1971**, *68*(*9*), 2236-2240.
9. Shepp L A, Logan B F. The Fourier reconstruction of a head section. *IEEE Transactions on Nuclear Science*, **2013**, *21*(*3*), 21-43.
10. Ramachandrana G N, Lakshminarayanan A V, Kolaskara A S. Theory of the non-planar peptide unit. *Biochimica et Biophysica Acta* (*BBA*)-*Protein Structure*, **1973**, *303*(*1*), 8-13.
11. Ludwig J, Mertelmeier T, Kunze H, et al. A novel approach for filtered backprojection in tomosynthesis based on filter kernels determined by iterative reconstruction techniques. In Proceedings of the *International Workshop on Digital Mammography*. Springer: Berlin/Heidelberg, Germany, 2008.
12. Shi H, Luo S. A novel scheme to design the filter for CT reconstruction using FBP algorithm. *Biomedical engineering online*, **2013**, *12*(*1*), 1-15.
13. Syben C, Stimpel B, Breininger K, et al. Precision Learning: Reconstruction Filter Kernel Discretization. *arXiv e-prints*, **2017**, arXiv-1710.
14. Kammler D W. *A first course in Fourier analysis*; Cambridge University Press: Cambridge, UK, 2007.
15. Bracewell R N. Strip integration in radio astronomy. *Australian Journal of Physics*, **1956**, *9*(2), 198-217.
16. Wei Y C, Wang G, Hsieh J. An intuitive discussion on the ideal ramp filter in computed tomography. *Computers & Mathematics with Applications*, **2005**, *49*(*5*), 731-740.